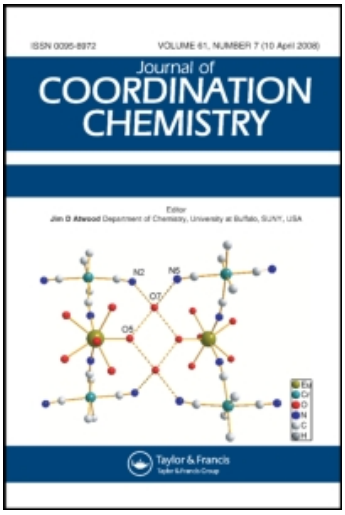

Journal of Coordination Chemistry
Publication details, including instructions for authors and subscription information:
http://www.informaworld.com/smpp/title~content=t713455674

Synthesis and characterization of 1',1'''-bis(ethynyl)biferrocenyl derivatives

Li-Min Han[a]; Yu-Qiang Hu[a]; Quan-Ling Suo[a]; Mei-Hua Luo[a]; Lin-Hong Weng[b]
[a] Chemical Engineering College, Inner Mongolia University of Technology, Hohhot 010051, P.R. China
[b] Department of Chemistry, Fudan University, Shanghai 200433, P.R. China

First published on: 10 February 2010

To cite this Article Han, Li-Min , Hu, Yu-Qiang , Suo, Quan-Ling , Luo, Mei-Hua and Weng, Lin-Hong(2010) 'Synthesis and characterization of 1',1'''-bis(ethynyl)biferrocenyl derivatives', Journal of Coordination Chemistry, 63: 4, 600 — 609, First published on: 10 February 2010 (iFirst)
To link to this Article: DOI: 10.1080/00958970903582688
URL: http://dx.doi.org/10.1080/00958970903582688

Journal of Coordination Chemistry
Vol. 63, No. 4, 20 February 2010, 600–609

Taylor & Francis
Taylor & Francis Group

Synthesis and characterization of 1′,1‴-bis(ethynyl)biferrocenyl derivatives

LI-MIN HAN*†, YU-QIANG HU†, QUAN-LING SUO*†, MEI-HUA LUO† and LIN-HONG WENG‡

†Chemical Engineering College, Inner Mongolia University of Technology, Hohhot 010051, P.R. China
‡Department of Chemistry, Fudan University, Shanghai 200433, P.R. China

(*Received 28 July 2009; in final form 24 September 2009*)

Three alkynylbiferrocenyl derivatives (**1**–**3**) were synthesized by cross coupling of 1′,1‴-diiodobiferrocene with the corresponding alkynyl cuprous species and characterized by elemental analysis, FT-IR, NMR, and MS. The molecular structures of $C_6H_5C{\equiv}CFc'Fc'C{\equiv}CC_6H_5$ (**1**), NO_2–$C_6H_4C{\equiv}CFc'Fc'C{\equiv}CC_6H_4$–$NO_2$ (**2**), and I–Fc′Fc′C≡CC_6H_4Fc (**3**) have been identified by X-ray single crystal diffraction. The electrode reaction processes of **1**–**3** were investigated by cyclic voltammetry, square wave voltammetry, and microelectrode chronoamperometry.

Keywords: Biferrocene; Cross coupling reaction; Molecular structure; Electron transfer

1. Introduction

Multi-redox-center molecules, especially biferrocenyl derivatives, have attracted considerable interest because of their potential applications as electron reservoirs and molecular electronic devices [1–3]. Potential applications are based on mixed-valence behavior and electron-transfer character between ferrocenyl groups [4]. Electrochemistry has been used (commonly cyclic voltammetry) to investigate ferrocenyl–ferrocenyl interactions [5]. The magnitude of the difference ($\Delta E_{1/2}$) of the half-wave potentials ($E_{1/2}$) between two redox waves gives an indication of the interaction between the metal sites, the larger the $\Delta E_{1/2}$ value, the greater the ferrocenyl–ferrocenyl interactions. The value of $\Delta E_{1/2}$ depends on the separation between the ferrocenyl centers and the degree of conjugation in the spacer linking the ferrocenyls [6]. However, the rate of intramolecular electronic communication and the number of electron transfers in mixed-valence biferrocenium cations can be controlled by environmental factors [7–12]; while more ferrocenyl are accumulated in one molecule, the electrode reaction processes and electron transfer numbers will be more complicated. How to identify the electron transfer numbers and electrode reaction processes of multi-ferrocenyl derivatives are hot research topics.

*Corresponding author. Email: hanlimin_442@hotmail.com (L.-M. Han); szj@imut.edu.cn (Q.-L. Suo)

Journal of Coordination Chemistry
ISSN 0095-8972 print/ISSN 1029-0389 online © 2010 Taylor & Francis
DOI: 10.1080/00958970903582688

Herein, we report the synthesis, molecular structures, electrode reaction processes, and the identification methods of electron transfer numbers of three biferrocenyl derivatives.

2. Experimental

2.1. *General procedures*

All manipulations were carried out using standard Schlenk techniques under an atmosphere of pure argon. Solvents were purified, dried, and distilled under an atmosphere of argon. Reactions were monitored by thin layer chromatography (TLC). Chromatographic separations and purification were performed on 200–300 mesh silica gel and neutral alumina.

1′,1‴-Diiodobiferrocene [13], copper(I) phenylacetylide [14], copper(I) *p*-nitrylphenyl acetylide, and copper(I) *p*-ferrocenylphenylacetylide [15, 16] were prepared according to literature methods. All other chemicals were purchased from Alfa Aesar.

IR spectra were recorded on a Nicolet FT-IR spectrometer in KBr disks. Elemental analyses were carried out on an Elementar vario III-type analyzer. ^{1}H and ^{13}C-NMR spectra in $CDCl_3$ were recorded on an Inova-500 MHz spectrometer. Mass spectra were determined using a Micromass LCT instrument. Melting points were determined by Autospec Ultima-TOF and JMS-T100LC instruments.

The platinum disks (radius 25 μm and 1.6 mm) were purchased from BAS and used as working electrodes for cyclic voltammetry, square wave voltammetry, and microelectrode chronoamperometry. The electrode surface was polished with 0.05 μm alumina before each run. The auxiliary electrode was a coiled platinum wire. The reference electrode was a Ag|AgCl electrode. The supporting electrolyte used in all electrochemical experiments was tetra-*n*-butylammonium hexafluorophosphate (TBAHFP). The potentiostat was a CHI-760C. Oxygen was purged from the one-compartment cell before electrochemical runs.

2.2. *Synthesis of C_6H_5–C≡C–Fc–Fc–C≡C–C_6H_5 (1)*

1′,1‴-Diiodobiferrocene (144.4 mg, 0.2323 mmol), PhC≡CCu (96.2 mg, 0.5806 mmol) and 50 mL dried pyridine were added to a 100 mL Schlenk flask. The solution was stirred for 4 h at 109°C, then cooled to room temperature. The solvent removed in vacuo yielded red oil. The residue was subjected to chromatographic separation on a neutral alumina column (2 × 35 cm). Elution with a mixture of hexane-dichloromethane (4 : 1 for **1a**; 3 : 1 for **1b**, v/v) afforded a red band for **1**. The single crystal of **1** was obtained by recrystallizing from hexane-dichloromethane (4 : 1, v/v) at room temperature. Compound **1**: Yield: 35.7%. m.p. 158–159°C. Anal. Calcd for $C_{36}H_{26}Fe_2$: C, 75.01; H, 4.51. Found: C, 75.81; H, 4.59%. IR (KBr disk): 2207.7 cm^{-1} (s) [$\nu_{C\equiv C}$]. ^{1}H-NMR ($CDCl_3$, δ): 7.28–7.43 (m, 10H, C_6H_5), 4.10–4.48 (m, 16H, Cp). ^{13}C-NMR ($CDCl_3$, δ): 123.97, 127.56, 128.17, 131.47 (C_6H_5), 86.23, 87.95 (C≡C), 68.19, 70.16, 70.35, 72.75 (Cp). MS (ESI, relative abundance): 570 (M^+, 100%).

2.3. *Synthesis of NO_2–C_6H_4–C≡C–Fc–Fc–C≡C–C_6H_4–NO_2 (2)*

1′,1′-Diiodobiferrocene (143.9 mg, 0.2315 mmol), *p*-NO_2PhC≡CCu (121.4 mg, 0.5786 mmol) and 50 mL dried pyridine were added to a 100 mL Schlenk flask. The solution was stirred for 4 h at 109°C, then cooled to room temperature. The solvents removed in vacuo yielded dark red oil. The residue was subjected to chromatographic separation on neutral alumina (2.0 × 35 cm). Elution with a mixture of hexane-dichloromethane (3 : 1, v/v) afforded a violet band for **2**. Violet crystals of **2** were obtained by recrystallizing from hexane-dichloromethane (4 : 1,v/v) at room temperature. Compound **2**: Yield: 44.9%. m.p. 254–255°C. Anal. Calcd for $C_{36}H_{24}O_4N_2Fe_2$: C, 65.10; H, 3.63; N, 3.96. Found: C, 65.49; H, 3.66; N, 4.24%. IR (KBr disk): 2197.4 cm^{-1} (m) [$\nu_{C\equiv C}$], 1588.0 cm^{-1} (m) [ν_{NO_2}]. ^{1}H-NMR ($CDCl_3$, δ): 7.46–8.16(m, 8H, C_6H_4), 4.15–4.41(m, 16H, Cp). ^{13}C-NMR ($CDCl_3$, δ): 123.54, 131.67 (C_6H_4), 86.231, 87.985 (C≡C), 68.02, 69.65, 70.61, 72.93 (Cp). MS (ESI, relative abundance): 660.10 (M^+, 100%).

2.4. *Synthesis of I–Fc–Fc–C≡C–C_6H_4–Fc (3)*

1′,1‴-Diiodobiferrocene (144.2 mg, 0.2323 mmol), p-FcPhCCCu (160.1 mg, 0.5868 mmol) and 50 mL dried pyridine were added to a 100 mL Schlenk flask. The solution was stirred for 8 h at 109°C, then cooled to room temperature. Removing solvent in vacuo yielded red oil. The residue was subjected to chromatographic separation on neutral alumina (2.0 × 30 cm^2). Elution with a mixture of hexane-dichloromethane (4 : 1, v/v) afforded an orange band for **3**. Red crystals of **3** were obtained by recrystallizing from hexane-dichloromethane (4 : 1, v/v) at room temperature. Compound **3**: Yield: 28.0%. m.p. 214–215°C. Anal. Calcd for $C_{38}H_{29}Fe_3I$: C, 59.04; H, 3.47. Found: C, 58.58; H, 3.75%. IR (KBr disk): 2202.6 cm^{-1} (m) [$\nu_{C\equiv C}$]. ^{1}H-NMR ($CDCl_3$, δ): 7.35–7.43 (m, 4H, C_6H_4), 3.98–4.67 (m, 25H, Cp). ^{13}C-NMR ($CDCl_3$, δ): 121.16, 125.73, 131.46, 139.08 (C_6H_4), 86.52, 87.97 (C≡C), 66.50, 68.45, 69.32, 69.54, 69.76, 69.92, 70.07, 70.20, 70.21, 71.00, 72.72 (Cp). MS (ESI, relative abundance): 780.00 (M^+, 100%).

3. Results and discussions

3.1. *Reaction and characterization of 1–3*

The reactions carried out in this work are summarized in Scheme 1. Compounds **1**–**3** were synthesized by cross-coupling of 1′,1‴-diiodobiferrocene with the corresponding alkynyl cuprous species. The three compounds were confirmed by FT-IR, ^{1}H-NMR, ^{13}C-NMR, elemental analysis, and MS.

3.2. *Molecular structures of 1–3*

Molecular structures of **1**, **2**, and **3** were determined by X-ray single crystal diffraction. Crystal data and relevant structural parameters were enumerated in table 1. The molecular structure of **1** is shown in figure 1 and selected bond lengths and angles are

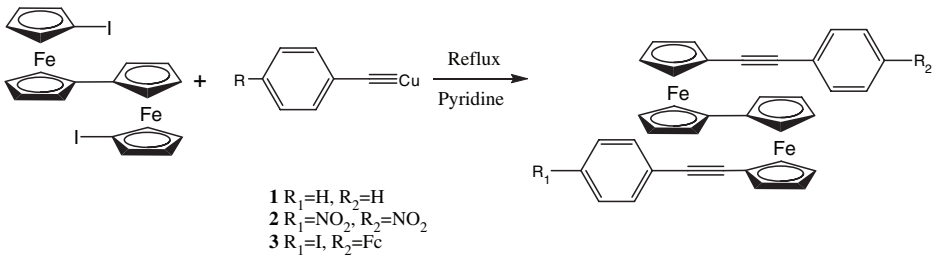

1 R_1=H, R_2=H
2 R_1=NO_2, R_2=NO_2
3 R_1=I, R_2=Fc

Scheme 1. The synthesis reaction of compounds **1**, **2**, and **3**.

Table 1. Crystallographic data and relevant structural parameters of **1**, **2**, and **3**.

Compounds	**1**	**2**	**3**
Empirical formula	$C_{36}H_{26}Fe_2$	$C_{36}H_{24}Fe_2N_2O_4$	$C_{38}H_{29}Fe_3I$
Crystal system	Monoclinic	Triclinic	Monoclinic
Space group	*P2(1)/c*	*P-1*	*P2(1)/c*
Unit cell dimensions (Å, °)			
a	12.875(4)	5.918(3)	15.300(6)
b	7.480(2)	10.951(5)	24.567(10)
c	14.782(5)	11.070(5)	7.932(3)
α	90	98.947(6)	90
β	110.594(5)	98.612(6)	92.634(6)
γ	90	91.900(6)	90
Volume (Å^3), *Z*	1332.6(7), 2	699.6(6), 1	2978(2), 4
Calculated density (g cm^{-3})	1.421	1.567	1.740
Absorption coefficient (mm^{-1})	1.112	1.083	2.506
F(000)	588	338	1552
θ range for data collection (°)	1.69–26.01	1.89–25.00	1.33–26.00
Reflections collected	5950	2902	13382
Independent reflections	2614	2404	5847
Completeness to $\theta = 25.02$ (%)	26.01	25.00	26.00
Max. and min. transmission	0.9163 and 0.8509	0.9478 and 0.7735	0.8850 and 0.6612
Data/restraints/parameters	2614/0/172	2404/0/199	5847/0/374
Goodness-of-fit on F^2	0.972	1.003	0.749
Final *R* indices [$I > 2\sigma(I)$]	$R_1 = 0.0525$, $wR_2 = 0.1179$	$R_1 = 0.0453$, $wR_2 = 0.1151$	$R_1 = 0.0512$, $wR_2 = 0.1322$
R indices (all data)	$R_1 = 0.0839$, $wR_2 = 0.1337$	$R_1 = 0.0513$, $wR_2 = 0.1171$	$R_1 = 0.0953$, $wR_2 = 0.1419$
Largest difference in peak and hole (e Å^{-3})	0.746 and −0.375	0.786 and −0.466	0.775 and −1.036

listed in table 2. The molecular structure of **2** is shown in figure 2 and selected bond lengths and angles are listed in table 3. The molecular structure of **3** is shown in figure 3 and selected bond lengths and angles listed in table 4.

Compound **1** contains biferrocenyl units in a *trans* conformation with the two irons on opposite sides of the planar fulvalenide bridge. The average distance from iron to the center of Cp rings is 1.641(1) Å, close to the Fe–Cp distance 1.65 Å found in ferrocene. The distance of C(10)–C(11) is 1.428(6) Å and C(12)–C(13) is 1.433(6) Å, both shorter than normal alkyl bonds. The angle of C(12)–C(11)–C(10) is 178.0(4)° and C(11)–C(12)–C(13) is 178.9(4)°, so C(10)–C(11)–C(12)–C(13) is nearly linear, and the dihedral of ferrocenyl plane to phenyl plane is 14.58°, indicating a conjugated system exists and the redox potential of ferrocenyl must be influenced by the phenyl.

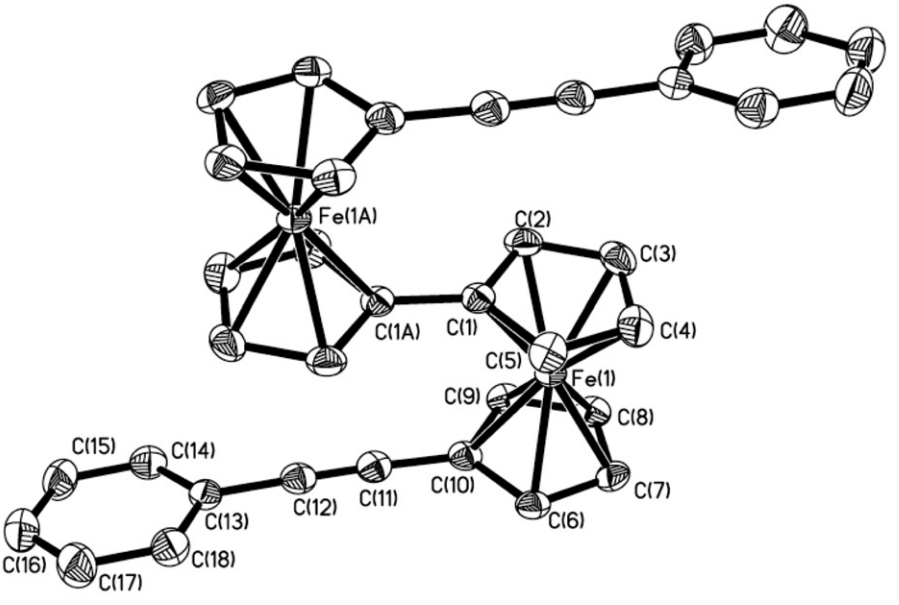

Figure 1. The molecular structure of **1**.

Table 2. Selected bond lengths (Å) and angles (°) for **1**.

Bond lengths				Bond angles			
C(1)−C(2)	1.415(5)	C(9)–C(10)	1.420(5)	C(2)−C(1)−C(5)	107.2(3)	C(9)−C(10)−C(11)	128.2(4)
C(1)−C(5)	1.418(5)	C(10)−C(11)	1.428(6)	C(2)−C(1)−C(1)$^{\#1}$	126.0(4)	C(6)−C(10)−C(11)	124.1(4)
C(1)−C(1a)	1.458(7)	C(11)−C(12)	1.179(5)	C(5)−C(1)−C(1)$^{\#1}$	126.8(4)	C(12)−C(11)−C(10)	178.0(4)
C(2)−C(3)	1.413(6)	C(12)−C(13)	1.433(6)	C(3)−C(2)−C(1)	108.4(4)	C(18)−C(13)−C(14)	118.4(4)
C(3)−C(4)	1.405(6)	C(13)−C(18)	1.383(6)	C(3)−C(4)−C(5)	108.3(4)	C(18)−C(13)−C(12)	120.3(4)
C(4)−C(5)	1.408(6)	C(14)−C(15)	1.370(6)	C(4)−C(5)−C(1)	108.2(4)	C(14)−C(13)−C(12)	121.2(4)
C(6)−C(7)	1.409(6)	C(15)−C(16)	1.367(7)	C(6)−C(7)−C(8)	108.3(4)	C(15)−C(16)−C(17)	119.1(5)
C(6)−C(10)	1.426(5)	C(16)−C(17)	1.370(7)	C(8)−C(9)−C(10)	107.7(3)	C(18)−C(17)−C(16)	121.0(5)
C(7)−C(8)	1.410(6)	C(17)−C(18)	1.368(6)	C(9)−C(10)−C(6)	107.7(3)	C(17)−C(18)−C(13)	120.3(4)

Symmetry transformations used to generate equivalent atoms: #1, $-x+2$, $-y$, $-z+2$.

Compound **2** also contains a biferrocenyl unit in a *trans* conformation with the two irons on opposite sides of the planar fulvalenide bridge. The average distance from iron to the center of Cp rings is 1.640(1) Å. The distance of C(10)–C(11) is 1.415(5) Å and C(12)–C(13) is 1.422(5) Å, both shorter than normal alkyl bonds. C(10)–C(11)–C(12)–C(13) is also nearly linear with phenyl and ferrocenyl a π conjugate. The two nitro groups on the phenyl of **2** will make the redox potentials of ferrocenyl different than **1** and electron communication of the ferrocenyls will be reduced.

Compound **3** contains a biferrocenyl unit and a ferrocenyl unit with the biferrocene unit in a *trans* conformation. C(20)–C(21) is 1.381(8) Å and C(22)–C(23) is 1.479(9) Å, both shorter than the normal alkyl bond. C(10)–C(11)–C(12)–C(13) is linear. The dihedral angle of C(16)–C(17)–C(18)–C(19)–C(20) to C(23)–C(24)–C(25)–C(26)–C(27)–C(28) is about 84.0(1)°, indicating the phenyl plane lost its conjugation to the

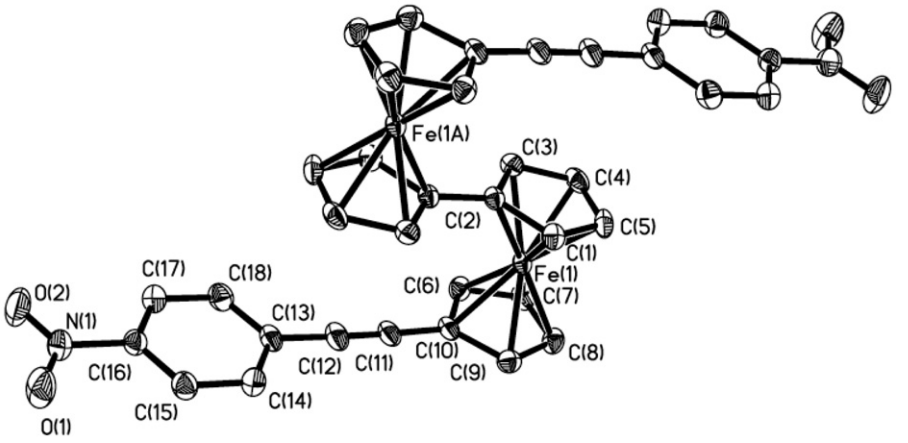

Figure 2. The molecular structure of **2.**

Table 3. Selected bond lengths (Å) and angles (°) for **2**.

Bond lengths				Bond angles			
C(1)–C(5)	1.427(5)	C(13)–C(18)	1.397(5)	C(9)–Fe(1)–C(4)	154.04(14)	C(11)–C(10)–C(6)	126.5(3)
C(1)—C(2)	1.433(4)	C(13)–C(14)	1.396(5)	C(9)–Fe(1)–C(6)	68.72(14)	C(12)–C(11)–C(10)	178.4(4)
C(2)–C(3)	1.423(5)	C(14)–C(15)	1.375(5)	C(4)–Fe(1)–C(6)	125.41(15)	C(18)–C(13)–C(14)	118.5(3)
C(2)–C(2)$^{\#1}$	1.453(6)	C(15)–C(16)	1.380(5)	C(9)–Fe(1)–C(5)	119.89(15)	C(14)–C(13)–C(12)	121.8(3)
C(3)–C(4)	1.413(5)	C(16)–C(17)	1.375(5)	C(4)–Fe(1)–C(5)	40.13(15)	C(15)–C(14)–C(13)	121.0(4)
C(4)–C(5)	1.402(5)	C(16)–N(1)	1.462(5)	C(6)–Fe(1)–C(5)	161.51(15)	C(14)–C(15)–C(16)	118.7(3)
C(6)–C(7)	1.417(5)	C(17)–C(18)	1.371(5)	C(4)–Fe(1)–C(3)	40.42(13)	C(17)–C(16)–N(1)	119.4(3)
C(6)–C(10)	1.431(5)	N(1)–O(2)	1.219(4)	C(6)–Fe(1)–C(3)	108.73(14)	C(15)–C(16)–N(1)	118.8(3)
C(7)–C(8)	1.404(5)	N(1)–O(1)	1.225(4)	C(5)–C(1)–C(2)	108.0(3)	C(17)–C(18)–C(13)	120.8(3)
C(9)–C(10)	1.434(5)	C(11)–C(12)	1.199(5)	C(3)–C(2)–C(2)$^{\#1}$	127.2(4)	O(2)–N(1)–O(1)	123.6(3)
C(10)–C(11)	1.415(5)	C(12)–C(13)	1.422(5)	C(1)–C(2)–C(2)$^{\#1}$	126.3(4)	O(1)–N(1)–C(16)	118.1(3)

Symmetry transformations used to generate equivalent atoms: #1, $-x+2$, $-y$, $-z+2$.

biferrocenyl unit; the dihedral angle of C(23)–C(24)–C(25)–C(26)–C(27)–C(28) to C(29)–C(30)–C(31)–C(32)–C(33) is about 6.60(1)° with conjugation between the ferrocenyl and phenyl. Hence, the effect of the phenyl on the redox potentials of ferrocenyl and biferrocenyl units is different.

3.3. *Electrochemistry*

The cyclic voltammograms (CV) of **1**, **2**, and **3** are provided in Supplementary material. The CV of **1** (curve *a*) displays two chemically reversible oxidation waves, each one-electron transfer, which can be assigned to two Fe(II)/Fe(III) redox couples. The oxidation potential difference (ΔE_a) between $E_{a,1}$ and $E_{a,2}$ of the ferrocenyl units is 350 mV, typical for biferrocene [17]. Comparing the CV of **2** to **1**, the redox potentials are shifted to more positive values, attributed to electron-withdrawing of nitro [18]. The oxidation potential difference (ΔE_b) between $E_{b,1}$ and $E_{b,2}$ of the ferrocenyl units is about 330 mV. Despite the comproportionation constant K_{cb} (3.8×10^5) being less

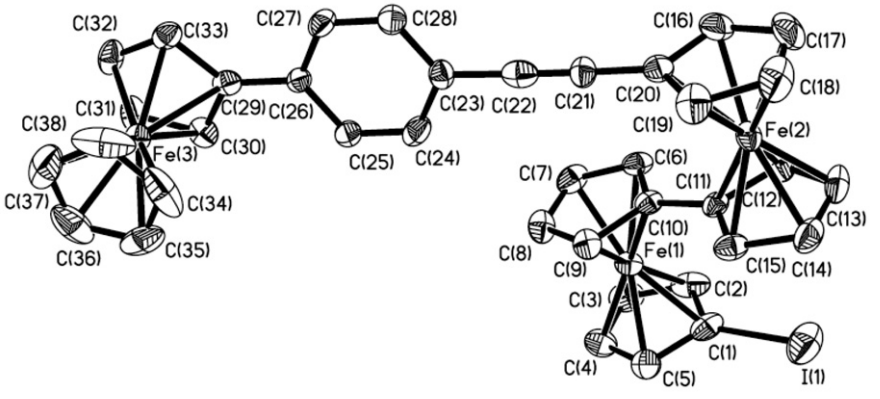

Figure 3. The molecular structure of **3**.

Table 4. Selected bond lengths (Å) and angles (°) for **3**.

Bond lengths				Bond angles			
I(1)–C(1)	2.092(7)	C(23)–C(28)	1.361(8)	C(2)–Fe(1)–C(9)	163.6(3)	C(15)–C(11)–C(10)	127.2(5)
C(1)–C(5)	1.447(9)	C(23)–C(24)	1.383(8)	C(2)–Fe(1)–C(1)	41.0(3)	C(21)–C(20)–C(19)	127.3(6)
C(1)–C(2)	1.416(9)	C(24)–C(25)	1.367(8)	C(9)–Fe(1)–C(1)	125.7(3)	C(21)–C(20)–C(16)	126.0(6)
C(2)–C(3)	1.388(9)	C(25)–C(26)	1.389(7)	C(2)–Fe(1)–C(5)	69.1(3)	C(21)–C(20)–Fe(2)	130.7(4)
C(3)–C(4)	1.360(9)	C(26)–C(29)	1.476(8)	C(9)–Fe(1)–C(5)	107.1(3)	C(22)–C(21)–C(20)	176.6(7)
C(6)–C(10)	1.403(8)	C(27)–C(28)	1.359(8)	C(1)–Fe(1)–C(5)	41.8(3)	C(21)–C(22)–C(23)	178.4(7)
C(6)–C(7)	1.420(8)	C(29)–C(33)	1.438(8)	C(9)–Fe(1)–C(4)	120.6(3)	C(28)–C(23)–C(22)	123.4(6)
C(7)–C(8)	1.388(9)	C(30)–C(31)	1.423(8)	C(5)–C(1)–C(2)	106.4(6)	C(28)–C(23)–C(24)	117.1(5)
C(9)–C(10)	1.423(8)	C(34)–C(38)	1.361(13)	C(5)–C(1)–I(1)	125.3(5)	C(27)–C(26)–C(29)	122.6(5)
C(11)–C(15)	1.417(8)	C(35)–C(36)	1.336(11)	C(2)–C(1)–I(1)	128.0(6)	C(25)–C(26)–C(29)	120.4(5)
C(11)–C(12)	1.433(8)	C(36)–C(37)	1.315(12)	Fe(1)–C(1)–I(1)	131.7(3)	C(33)–C(29)–C(26)	127.1(5)
C(13)–C(14)	1.401(9)	C(19)–C(20)	1.439(9)	C(3)–C(2)–C(1)	107.5(6)	C(30)–C(29)–C(26)	127.2(5)
C(14)–C(15)	1.419(8)	C(20)–C(21)	1.381(8)	C(3)–C(4)–C(5)	111.4(7)	C(30)–C(31)–C(32)	109.6(6)
C(16)–C(20)	1.423(8)	C(21)–C(22)	1.172(8)	C(4)–C(5)–C(1)	106.3(6)	C(38)–C(34)–C(35)	110.1(8)
C(18)–C(19)	1.427(9)	C(22)–C(23)	1.479(9)	C(9)–C(10)–C(11)	126.1(5)	C(11)–C(10)–Fe(1)	125.0(4)

than the K_{ca} (8.4×10^5), where $K_c = \mathrm{Exp}(nF\Delta E_b/RT)$, **2** is still a mixed-valence Fe(II)–Fe(III) species [19]. The electrode oxidation of **1** and **2** are shown in scheme 2 (processes a). The CV of **3** also exhibits two redox peaks rather than the predicted three. The peak current of the first oxidation peak is two times that of the second in the square wave voltammogram of **3** (figure 4), suggesting the first oxidation is a two-electron transfer.

The two-electron process of the first oxidation step of **3** can also be identified by microelectrode chronoamperometry. According to the documental methods [20–23], within diffusion controlled potential domain, the Cottrell Plot (I *vs.* $t^{-1/2}$) of **3** at a microelectrode gives the slope, s, and intercept, p, respectively (figure 5 and Supplementary material),

$$s = \pi^{1/2} n D^{1/2} F a^2 c^* (1 + e^{\varsigma})^{-1}, \quad p = \pi n F D a c^* (1 + e^{-\varsigma})^{-1},$$

where $\varsigma = (F/RT)(E - E^0)$, F is faradic constant, a the radius of microelectrode, and c^* the concentration of the solution. On the assumption of $\varsigma \to \infty$ from the ratio of s^2 to p,

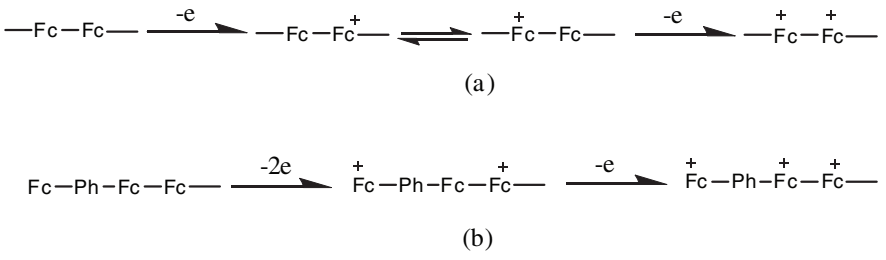

Scheme 2. The electrode reaction processes of compounds **1**, **2**, and **3**.

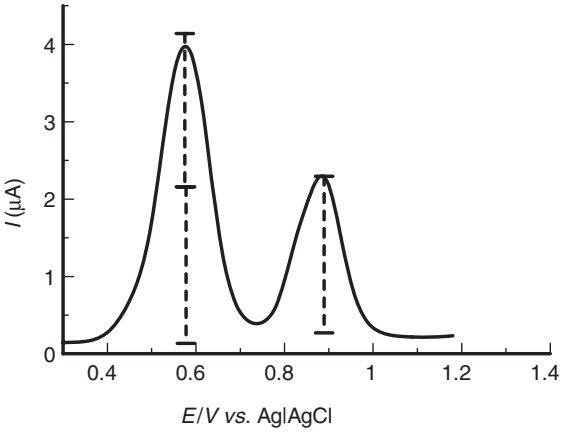

Figure 4. Square wave voltammogram of **3** in CH_2Cl_2 with TBAFP (0.5 M).

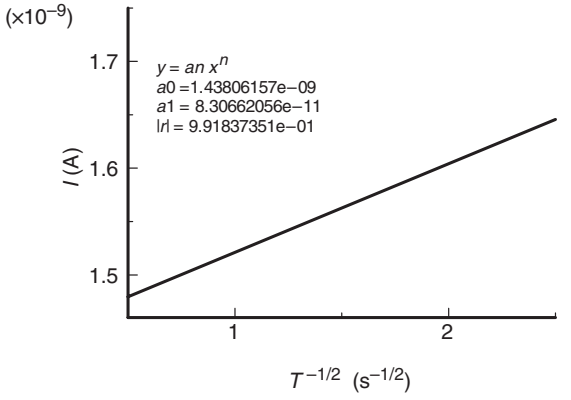

Figure 5. Cottrell plot of the background-sunstracted currents for 2.0 mM (**3**) in CH_2Cl_2 with TBAFP (0.5 M) when potential was stepped from 0.3 to 0.7 V.

the electron transfer number can be expressed as $n = s^2/pFa^3c^*$. The calculated electron transfer number (n) is approximate to 2, consistent with the suggested values of the square wave voltammogram. Electrode processes are depicted in scheme 2 (processes b). Compared to conventional cyclic voltammetric methods [24], the microelectrode

chronoamperometry is more precise for calculating the electron transfer numbers of ferrocenyl derivatives.

4. Conclusion

Three biferrocene derivatives, PhC≡CFc′Fc′C≡CPh (**1**), O_2NPhC≡CFc′Fc′C≡CPhNO_2 (**2**) and IFc′Fc′C≡CPhFc (**3**), have been synthesized by cross coupling of terminal copper(I) alkylide and 1′,1′-diiodobiferrocene and characterized by elemental analysis, FT-IR, NMR, and MS. The structures of **1**, **2**, and **3** have been determined by X-ray single crystal diffraction. The electrode reaction processes and electron transfer numbers of three compounds were investigated by cyclic voltammetry, square wave voltammetry, and microelectrode chronoamperometry.

Supplementary material

Crystallographic data for the structural analysis have been deposited at the Cambridge Crystallographic Data Centre, CCDC nos 742295, 742296, and 742297 for **1**, **2**, and **3**, respectively. The copies of this information may be obtained free of charge from the Director, CCDC, 12 Union Road, Cambridge CB2 1EZ, UK (Fax: +44-1223 336033; Email: deposit@ccdc.cam.ac.uk).

Acknowledgements

We are grateful to the Specialized Research Fund for the Doctoral Program of Higher Education of China (20060128001), the Program for New Century Excellent Talents in University (NCET-08-858), the Natural Science Foundation of the Inner Mongolia (20070128001) and (20080404MS020).

References

[1] J.B. Flanagan, S. Margel, A.J. Bard, F.C. Anson. *J. Am. Chem. Soc.*, **100**, 4248 (1978).
[2] A. Tarrasa, P. Molina, D. Curiel, M.D. Velasco. *Organometallics*, **20**, 2145 (2001).
[3] P.A. Chase, R.G. Gebbink, G. Van Koten. *J. Organomet. Chem.*, **689**, 4016 (2004).
[4] P. Shu, K. Bechgaard, D. Cowan. *J. Org. Chem.*, **10**, 1849 (1976).
[5] M. Neuburger, S. Schaffner, E.J. Shardlow. *Dalton Trans.*, 234 (2005).
[6] T.Y. Dong, T.J. Ke, S.M. Peng, S.K. Yeh. *Inorg. Chem.*, **28**, 2105 (1989).
[7] S. Nakashima, T. Oka, T. Okuda, M. Watanabe. *Inorg. Chem.*, **38**, 4005 (1999).
[8] M. Kai, M. Katada, H. Sano. *Chem. Lett.*, **17**, 1523 (1988).
[9] T.Y. Dong, C.C. Schei, T.L. Hsu, S.L. Lee, S.J. Li. *Inorg. Chem.*, **30**, 2457 (1991).
[10] T.Y. Dong, C.Y. Chou. *J. Chem. Soc., Chem. Commun.*, 1332 (1990).
[11] T.Y. Dong, C.C. Schei, M.Y. Hwang, T.Y. Lee, S.K. Yeh, Y.S. Wen. *Organometallics*, **11**, 573 (1992).
[12] R.J. Webb, T.Y. Dong, C.G. Pierpont, S.R. Boone, R.K. Chadha, D.N. Hendrickson. *J. Am. Chem. Soc.*, **113**, 4806 (1991).

[13] M. Rosenblum, N. Brawn, J. Papenmeier. *J. Organomet. Chem.*, **6**, 173 (1966).
[14] W.K. George, L. Wang, V. Namboodiri. *Tetrahedron Lett.*, **41**, 5151 (2000).
[15] L.Y. Wang, Q.L. Suo, L.M. Han. *Polyhedron*, **26**, 4981 (2007).
[16] N. Zhu, Q.L. Suo, Y.B. Wang. *Polyhedron*, **26**, 981 (2007).
[17] M.C.B. Colbert, D. Hodgson, J. Lewis, P.R. Raithby, N. Long. *Polyhedron*, **14**, 2759 (1995).
[18] T.Y. Dong, B.R. Huang, S.M. Peng, G.H. Lee, M.Y. Chiang. *J. Organomet. Chem.*, **659**, 125 (2002).
[19] J.E. Sutton, H. Taube. *Inorg. Chem.*, **20**, 3125 (1981).
[20] K. Aoki, J. Osteryoung. *J. Electroanal. Chem.*, **160**, 335 (1984).
[21] K. Aoki, J. Osteryoung. *J. Electroanal. Chem.*, **122**, 19 (1981).
[22] T. Nishiumi, M.M. Abdul. *Electrochem. Commun.*, **7**, 1213 (2005).
[23] L.M. Han, Q.L. Suo, M.H. Luo, N. Zhu, Y.Q. Ma. *Inorg. Chem. Commun.*, **11**, 873 (2008).
[24] Y.R. Liu, Z.Y. Cao, H.W. Hou, Y.T. Fan. *J. Coord. Chem.*, **62**, 277 (2009).